PHYSICAL REVIEW B **69**, 115335 (2004)

Anisotropic diffusion of In adatoms on pseudomorphic $In_xGa_{1-x}As$ films: First-principles total energy calculations

E. Penev, S. Stojković,* P. Kratzer, and M. Scheffler
Fritz-Haber-Institut der Max-Planck-Gesellschaft, Faradayweg 4-6, D-14195 Berlin-Dahlem, Germany
(Received 19 September 2003; published 26 March 2004)

In the Stranski-Krastanow growth of strained pseudomorphic films, material transport by surface diffusion plays a crucial role for the development of the three-dimensional island morphology. In an attempt to elucidate the atomistic aspects of this growth mode, we study diffusion of a single indium adatom on (1×3)- and (2×3)-reconstructed subcritical $In_{2/3}Ga_{1/3}As(001)$ films using first-principles total energy calculations of the corresponding adiabatic potential-energy surfaces (PES). We find that In diffusion is anisotropic, and substantially enhanced compared to the conventional GaAs(001)-$c(4\times4)$ substrate. Special attention is also paid to the methodology of deriving the tracer diffusion coefficients of indium from knowledge of the PES, using the continuous-time random-walk formalism.

DOI: 10.1103/PhysRevB.69.115335 PACS number(s): 68.43.Bc, 68.35.Fx, 68.65.−k

I. INTRODUCTION

Several technologically relevant processes in semiconductor fabrication are crucially affected by diffusion of adsorbed particles. Unfortunately, the understanding of the underlying physics of surface diffusion, island nucleation, and growth, which is relevant for predictive modeling of processing techniques and the function of materials, is still shallow. Also, atomic-scale experimental data are scarce. This is partly due to the fact that measurements of surface diffusivity are difficult, and mostly performed in an indirect way, i.e., by inferring the diffusion length from morphological quantities such as island or the step densities.[1,2] While some insight has been gained using direct probes, such as *in situ* scanning tunneling microscopy (STM),[3,4] the relatively high growth temperatures typically used in the molecular-beam epitaxy (MBE) of semiconductors often precludes the use of such probes under realistic conditions. In this situation, first-principles calculations can provide useful additional data. However, such studies are very elaborate, and, for example, require detailed knowledge of the surface reconstruction and its evolution during growth. Furthermore, reconstructions with large unit cells can result in a complex potential-energy surface for the diffusing adatom, and careful analysis of its implications for the kinetics of surface diffusion is required.

The latter point is the main topic of our paper that describes a theoretical analysis of surface diffusion of indium atoms during heteroepitaxy of InAs on the GaAs(001) substrate. While there is a large body of literature about surface diffusion in general (for a review, see Refs. 5 and 6), very little is known about diffusion of indium atoms on a GaAs substrate or on a pseudomorphic $In_xGa_{1-x}As(001)$ film. This material system, however, is of particular interest because it allows for the spontaneous formation of nanostructures[7–9] [three-dimensional (3D) islands that can be used as quantum dots after overgrowing them with a capping layer]. Both experimental and theoretical investigations agree that it is the surface diffusion of cations which is most important for the surface morphology in MBE of III-V compounds, whereas the kinetics of arsenic incorporation is dominated by direct adsorption and desorption of As dimers or tetramers.[10] It is well known experimentally that the aforementioned 3D heteroepitaxial islands only form after a certain critical deposition of InAs. For deposition of a smaller amount, a pseudomorphic film is formed, usually termed a wetting layer (WL). After a critical thickness θ_c of the WL is exceeded [typically 1.7 ± 0.3 monolayers (ML)], the formation of 3D islands proceeds very quickly, while at the same time material from the WL is consumed by this process, i.e., the wetting layer thickness is shrinking after the islands have appeared (see, for example, Ref. 11). Thus, the island formation requires considerable mass transfer by surface diffusion from the WL to the islands, as evidenced by several experiments.[12–18] The aim of the present study is to elucidate the underlying microscopic processes. As a first step in this direction, some of us have previously investigated the effect of strain on In diffusion on the GaAs(001)-$c(4\times4)$ surface.[19,20] The latter reconstruction is present on the GaAs substrate when depositing under As-rich conditions.[21,22] The next challenging question concerns the In diffusivity on the WL before the critical thickness is reached, i.e., for $\theta<\theta_c$.

Below we report density-functional-theory (DFT) calculations and an analysis for indium tracer diffusion on the WL. The extensive experimental data on the initial stages of InAs/GaAs(001) growth indicate that for conventional growth rates ($\simeq0.1$ ML/s) substantial alloying occurs which converts the WL into a ternary $In_xGa_{1-x}As(001)$ alloy exhibiting specific (1×3) or (2×3) reconstruction patterns.[23–25] Based on this information, some of us have recently studied the *ab initio* thermodynamics of the WL (Ref. 26) and found support for surface alloying for submonolayer InAs coverage under As-rich growth conditions. Theoretical structure analysis[27] showed that the (2×3) reconstruction can be regarded as the main building unit of such a WL. The geometry parameters are in very good agreement with the experimental x-ray analysis.[23,24,28] Reflection high-energy electron-diffraction (RHEED) data, on the other hand, have been interpreted as giving evidence for a (1×3) reconstruction. While DFT calculations[27] have shown that the (1×3) reconstruction has a higher surface energy than the (2×3) recon-

 ©2004 The American Physical Society

struction, it is conceivable that both reconstruction patterns are present simultaneously due to the experimental preparation conditions. In this work, we therefore employ both structural models of the $In_xGa_{1-x}As(001)$ WL to study indium adatom diffusion.

Technical details of the calculations are given in the following section. Indium diffusivity on both (1×3)- and (2×3)-reconstructed $In_xGa_{1-x}As(001)$ films is analyzed in Sec. III. In Sec. IV we compare it to In diffusion on the GaAs(001)-$c(4\times4)$ surface and discuss our results.

II. THEORETICAL SCHEME

The theoretical framework of the present study is identical to our previous work; for a detailed description and extensive discussion we refer the reader, e.g., to Refs. 29–31. In brief, we first performed total energy DFT calculations using the computer program FHI98MD (Ref. 32) to determine the adiabatic potential-energy surface (PES) for surface diffusion of an In adatom. Within the supercell approach, reconstructed surfaces are represented by slabs of seven atomic layers, whose bottom Ga-terminated surface is passivated by pseudo-H atoms ($Z=1.25$). In the (001) plane the actual size of the supercells is (4×3), i.e., in the $[\bar{1}10]$ direction it is a factor of 4 or 2 larger than the considered surface periodicity. This is needed to make the artificial adsorbate interaction negligible. In normal direction, the slabs are separated by a vacuum region corresponding to approximately six interlayer distances. Equilibrium surface geometries are obtained by atomic relaxation until the residual forces $\lesssim 0.025$ eV/Å, keeping the bottom layer and pseudo-H atoms fixed. Brillouin-zone (BZ) integration was carried out using a set of special **k** points equivalent to 72 points in the 1×1 surface BZ. Kohn-Sham orbitals were expanded in plane waves up to a cutoff energy of 10 Ry. The Perdew-Burke-Ernzerhof generalized gradient approximation[33] was employed to describe the electronic exchange and correlation interaction. *Ab initio* norm-conserving pseudopotentials are used for all species.[34] These were constructed using the highest s and p states of Ga, In, and As as valence states. For In, we also tested including $4d$ states in the valence shell, but found that this does not improve performance for InAs bulk properties. Therefore these states were finally also "hidden" in the pseudopotential.

With these settings, the PES is obtained by calculating the In binding energy E_b on a discrete grid of points $\{X,Y\}$ in the (001) plane in the symmetry-irreducible part of the supercell. As the energy zero we chose the sum of the total energies of the slab representing the clean surface plus the energy of an isolated spin-polarized In atom. For fixed (X,Y) the Z coordinate of the adatom is optimized starting from $\simeq 2$ Å above the surface, allowing also the topmost five atomic layers of the substrate to freely relax. The final "map" of the PES is obtained by exploiting surface symmetries and interpolating the calculated points with bicubic splines.[35]

In order to calculate the diffusion coefficient, we solve the master equation for a Markovian random walk on a discrete lattice. The minima and saddle points of the calculated potential-energy surface are mapped onto the nodes and interconnects of an infinite network, and we assume that the surface diffusion occurs via uncorrelated jumps between the nearest-neighbor adsorption sites $\mathbf{A}_i$ of the PES, i.e., "single" jumps. The rates Γ_{fi} for jumps from an initial site $\mathbf{A}_i$ to a final site $\mathbf{A}_f$, crossing the saddle point $\mathbf{T}_k$, are calculated within transition state theory according to

$$\Gamma_{fi}=\Gamma_{fi}^0\exp(-\epsilon), \quad \epsilon\equiv\frac{\Delta E}{k_B T}, \tag{1}$$

where $\Delta E=E_b(\mathbf{T}_k)-E_b(\mathbf{A}_i)$ is the adiabatic barrier, k_B the Boltzmann constant, and T the substrate temperature (for a discussion of the underlying assumptions see, e.g., Refs. 36 and 6). Frequency prefactors Γ_{fi}^0 are estimated within the harmonic approximation for the lattice vibrations with a force-constant matrix including only the adatom degrees of freedom. Previous work[37] has demonstrated that this is an acceptable approximation for the dynamical matrix. Indeed, at least for the particular case of Ag hopping diffusion on Ag(111), the tests in Ref. 37 including between 3 and $\simeq 100$ degrees of freedom resulted in Γ^0 variations within only a factor of 2. Furthermore, one can expect that the ratios of prefactors come out more precisely than their absolute values, since only processes of the same kind (jumps) are considered. Note, however, that accurate energy barriers are more important for the following analysis as they enter the activation exponent in Eq. (1).

The applicability of the single jump description requires the energy scale set by the growth temperature (typically $k_B T\sim 60$ meV) to be sufficiently smaller than the energy barriers,

$$\epsilon \gg 1. \tag{2}$$

As it will be shown below, for some transitions $\epsilon\sim 1$, thus violating condition (2). Hence, the actual diffusion regime is also determined by the energy dissipation due to the frictional coupling of the adatom to the substrate. Comprehensive studies of different regimes are available in the literature,[6,36,38–40] an important implication being the possibility for an adatom to commit *longer* jumps given a low-to-moderate friction.[41] Here we shall not attempt a quantitative discussion on the frictional damping. Instead, a phenomenological approach is adopted to get some insight into the effect of possible "*double*" jumps in the (lattice) random-walk formalism.[42] Further details are given in the following section.

Finally, the indium tracer diffusion tensor D is obtained by solving the master equation for the corresponding network of sites in the long-time limit (see the Appendixes).[43] This method has been previously applied to adatom diffusion on stepped surfaces,[44] Ga diffusion on GaAs(001)-$\beta 2(2\times4)$, Ref. 45, and In diffusion on GaAs(001)-$c(4\times4)$, Ref. 19.

III. TRACER DIFFUSION ON A PSEUDOMORPHIC $In_{2/3}Ga_{1/3}As(001)$ FILM

Various surface phases for the WL, depending on indium coverage and preparation temperature, have been reported in

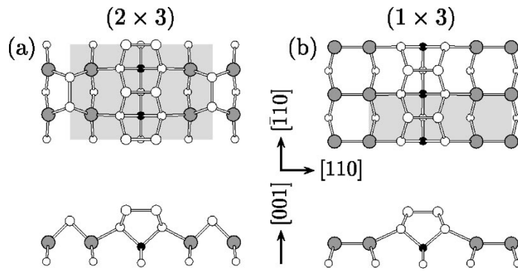

FIG. 1. Structural models for the reconstructions of the $In_{2/3}Ga_{1/3}As(001)$ surface. Shaded polygons represent the surface unit cell. The atomic arrangement is indicated for atoms in the topmost four atomic layers (In, gray circles; Ga, black circles; As, open circles). Side views are shown in the lower parts of the panels.

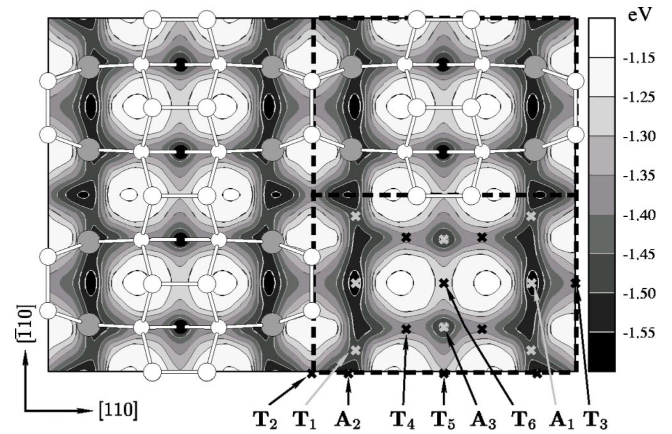

FIG. 2. PES for an In adatom on the $In_{2/3}Ga_{1/3}As(001)$-(2×3) surface, see also Table I. Two unit cells are indicated by dashed rectangles. Overlaid on the PES plot are the topmost three atomic layers of the clean surface (cf. Fig. 1).

combined STM and RHEED experiments.[25] As mentioned in the Introduction, we will focus on In migration under those conditions where alloying in the WL leads to a surface atomic arrangement with threefold periodicity along the [110] surface direction. More precisely, we study surface diffusion on two idealized surfaces with a (2×3) and a (1×3) reconstruction pattern. While these surfaces do not exactly represent the typical wetting layer encountered in experiments, they allow us to address the effect of alloying on the diffusivity by comparing to our previous results, in particular to those for In diffusion on GaAs(001)-$c(4\times4)$.

Our choice of the atomic structures for the $In_xGa_{1-x}As(001)$ alloy surface was motivated by experimental information using several probes. Sauvage-Simkin *et al.*[24] and Garreau *et al.*[28] concluded from their analysis of x-ray-diffraction data that well-developed periodicity of three lattice constants in [110] direction correlates with an In concentration of $x=2/3$ in the first subsurface cation layer. They concluded that cation ordering stabilizes a (2×3) reconstruction under As-rich conditions, and came up with the structural model for $In_{2/3}Ga_{1/3}As(001)$-(2×3) shown in Fig. 1(a). DFT calculations[27,26,46] supported this model by demonstrating that it is energetically preferred among several other surface reconstructions, and finding good agreement between calculated atomic positions and those derived from the x-ray data. This (2×3) reconstruction is characterized by continuous top-layer rows of As dimers running along the $[\bar{1}10]$ direction. In the third layer, four out of six cation positions are occupied by In and 2 by Ga atoms, the latter preferentially occupying the site below the As dimers. The twofold periodicity along $[\bar{1}10]$ is due to the structural motif comprising an As dimer back-bonded to the four third-layer In atoms. Very recently, reflectance-difference spectroscopy and RHEED experiments[47] demonstrated that the (2×3) reconstruction may even persist up to θ_c for relatively low T. Hence, in Sec. III A, we will first consider indium diffusion on the $In_{2/3}Ga_{1/3}As(001)$-(2×3) surface. Then, in Sec. III B, a corresponding study is performed for In on the $In_{2/3}Ga_{1/3}As(001)$-(1×3) surface. The (1×3) structural model, Fig. 1(b), was invoked to rationalize the commonly observed RHEED patterns of this symmetry in the very early stages of InAs deposition. One can think of this model as being derived from the (2×3) reconstruction by removing the As dimers with bonds aligned in $[\bar{1}10]$ direction, and dimerizing the exposed In atoms along the [110] direction. In support of this structure, Kita *et al.*[47] inferred the presence of In-In bonds from spectroscopic data, by analogy to similar studies on the Ga-rich GaAs(001)-(4×2) surface.[48] However, first-principles studies[27,31] find the (1×3) reconstruction to be higher in energy than the (2×3) reconstruction for arsenic-rich conditions. Concluding from these calculations, one would not expect the (1×3) reconstruction as a stable equilibrium structure under any conditions. However, experimental data suggest that it may be present locally on the surface of $In_xGa_{1-x}As(001)$ films as an element of frozen-in structural disorder. Hence we include this surface in our diffusion study.

A. In adatom on $In_{2/3}Ga_{1/3}As(001)$-(2×3)

In this section, we will determine the tracer diffusion coefficients for In on the (2×3) reconstructed $In_{2/3}Ga_{1/3}As(001)$ surface. As a first step, we create a map of the PES. Because of the two mirror planes in the (2×3) unit cell, only 1/4 of it needs to be sampled, and for this region, we use a uniform grid of 35 points. The resulting PES is shown in Fig. 2, and the energies for significant points are collected in Table I.

The corrugation of this PES is remarkably small: The maximum variation of the adiabatic potential in the (001) plane is $\simeq 0.5$ eV. We find three symmetry-inequivalent potential minima and six saddle points: The energy barriers are all smaller than 0.3 eV. The adsorption site providing strongest binding, $\mathbf{A}_1$, is located between a top-layer As dimer and the As dimer bound to the third-layer In atoms. Another adsorption site $\mathbf{A}_2$ appears next to a top-layer As dimer, but located in the gap between two As dimers bound to the third-layer In atoms. The troughs in the continuous As dimer row in $[\bar{1}10]$ direction give rise to a shallower site $\mathbf{A}_3$.

Similar to previous work,[10,19,45,49] for a valid description of In diffusion by the PES shown in Fig. 2, we find it necessary to check if interaction of In with the As-As bonds can

TABLE I. Binding energy E_b (eV) of an In adatom at the potential minima $\mathbf{A}_i$ and saddle points $\mathbf{T}_k$ found on the PES in Fig. 2.

	Site								
	$\mathbf{A}_1$	$\mathbf{A}_2$	$\mathbf{A}_3$	$\mathbf{T}_1$	$\mathbf{T}_2$	$\mathbf{T}_3$	$\mathbf{T}_4$	$\mathbf{T}_5$	$\mathbf{T}_6$
E_b	−1.61	−1.56	−1.46	−1.48	−1.39	−1.37	−1.32	−1.29	−1.27

lead to more stable binding sites for In than the minima of the PES. Indeed, locating the strongest binding site for a given lateral position (X,Y) of the adatom, with no other constraints, poses a multidimensional minimization problem. Relaxation starting from a given initial configuration may only lead to a *local* minimum, even if all degrees of freedom of the substrate atoms are relaxed. However, the global minimum of the binding energy for given lateral position (X,Y) of the adatom is required. In the case of several minima [e.g., one for the adatom sitting above an As dimer, Fig. 3(a), another for the adatom located inside the As dimer, Fig. 3(c)], all of them must be considered. This is why, in addition to just relaxing from a starting geometry with the adatom above the surface, we also perform a search for further binding sites.

To this end, we have recalculated E_b at the $\mathbf{T}_3$, $\mathbf{T}_5$, and $\mathbf{T}_6$ sites starting from an initial geometry, Fig. 3(c), where the corresponding As dimer is split to accommodate the In adatom. As a result, it was found that dimer splitting indeed lowered the energy at the $\mathbf{T}_3$ site to $E_b=-1.5$ eV, but such an effect was not present for either of the $\mathbf{T}_5$ and $\mathbf{T}_6$ sites related to the As dimers in the topmost layer. The importance of the indium interaction with the As dimer at the $\mathbf{T}_3$ site is determined by the accessibility of the binding configuration shown in Fig. 3(c). However we find this process to be activated, with an energy barrier of $\simeq 0.5$ eV needed for the adatom to reach the more stable configuration, Fig. 3(c), starting from that of the $\mathbf{T}_3$ site, Fig. 3(a). The search for the saddle point has been carried out by means of the ridge method,[50] and the transition-state geometry is shown in Fig. 3(b). The calculated barrier is by $\simeq 0.2$ eV higher than the maximum diffusion barrier on the (2×3) PES, Fig. 2. Thus, for the temperatures of interest, this energy characteristic disqualifies the interaction of In with the "trench" As dimer from the list of important processes when considering In surface diffusion.

The energy barriers ΔE for single jumps between the potential minima in Fig. 2 are directly obtained from Table I and are given in Table II along with the corresponding calculated prefactors Γ^0_{fi}. As already suggested by the PES plot of Fig. 2, also the results of Table II imply that the In migration on the $In_{2/3}Ga_{1/3}As(001)$-(2×3) pseudomorphic film is expected to be strongly anisotropic. The "fast" $[\bar{1}10]$ direction is associated with jumps between the $\mathbf{A}_1$ and $\mathbf{A}_2$ sites and the effective diffusion barrier is determined by the higher of the two activation energies, $\Delta E^{\mathrm{eff}}_{[\bar{1}10]}=\Delta E_{21}=0.13$ eV (cf. Table II). Similarly, along the "slow" $[110]$ direction, across the continuous dimer row, the rate-limiting transition is from $\mathbf{A}_1$ to $\mathbf{A}_3$, and thus $\Delta E^{\mathrm{eff}}_{[110]}=\Delta E_{31}\simeq 0.3$ eV. These simple estimates are corroborated by the analytical expressions obtained from the random-walk (RW) formalism (Appendix A).

The 2D lattice walk by single jumps associated with the (2×3) PES is sketched in Fig. 4. Then from Eq. (A9) in Appendix A, and using Eq. (1) and Table II to evaluate the jump rates, we obtain the diffusion tensor. For example, for $T\sim 620$ K, $D_{[110]}\simeq 9\times10^{-6}$ cm^2/s and $D_{[\bar{1}10]}\simeq 10^{-4}$ cm^2/s, which gives an estimate for the diffusion anisotropy in this low-temperature regime,

$$D_{[110]}/D_{[\bar{1}10]}\sim 0.1. \tag{3}$$

At elevated temperature ($\epsilon \gtrsim 1$) and low-to-moderate friction, a simple analysis on the basis of single jumps is not fully adequate, because the potential minimum at $\mathbf{A}_2$ may no longer serve as a trap. Indium atoms diffusing along the trenches in $[\bar{1}10]$ direction by the jump sequence $\mathbf{A}_1\rightarrow\mathbf{A}_2\rightarrow\mathbf{A}_1$ will not equilibrate in $\mathbf{A}_2$, but continue to move to the adjacent $\mathbf{A}_1$ site, i.e., they will effectively perform double jumps $\mathbf{A}_1\rightarrow\mathbf{A}_1$. Higher-order jumps (i.e., "triple" jumps) need not be considered, because their probabilities are exponentially small. In fact, the abundance of long jumps in this case, if possible at all, may be substantially reduced due to the nonrectilinear path along the trenches,[6] cf. Figs. 2 and 4. Methods to work out the rate $\tilde{\Gamma}_{11}$ for double jumps, e.g., by molecular dynamics, have been described in the literature. It has been found[38–40] that it obeys an Arrhenius-type law similar to Eq. (1), with an additional activation energy[38] δ in excess of the potential-energy barrier ΔE, and a prefactor

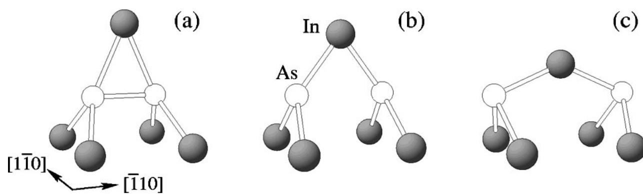

FIG. 3. Bonding configurations for (a) In at the $\mathbf{T}_3$ site on the PES from Fig. 2; (b) at the transition state, before splitting the As dimer, and (c) In splitting the As dimer.

TABLE II. Energy barriers ΔE (in eV, according to Table I) and attempt frequencies Γ^0_{fi} (THz) for single jumps.

	$fi(\mathbf{A}_i\rightarrow\mathbf{A}_f)$						
	11	12	21	22	13	31	33
ΔE	0.24	0.08	0.13	0.17	0.14	0.29	0.18
Γ^0_{fi}	0.7	0.3	0.8	0.5	1.0	0.6	0.8

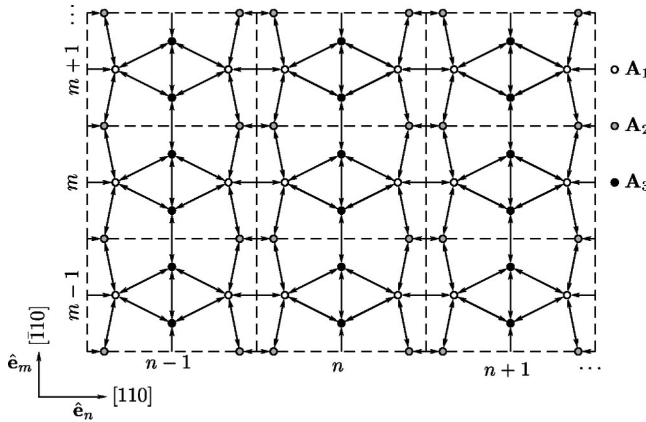

FIG. 4. Network of binding sites and possible single jumps for an In adatom on the $In_{2/3}Ga_{1/3}As(001)$-(2×3) surface used in the random-walk formalism. There are $N_b=6$ binding sites per unit cell. The lattice coordinate basis is $\{\hat{\mathbf{e}}_n,\hat{\mathbf{e}}_m\}$, and the unit cells (dashed rectangles) are labeled by a vector index $\mathbf{n}=(n,m)$ with $n,m=$ integer.

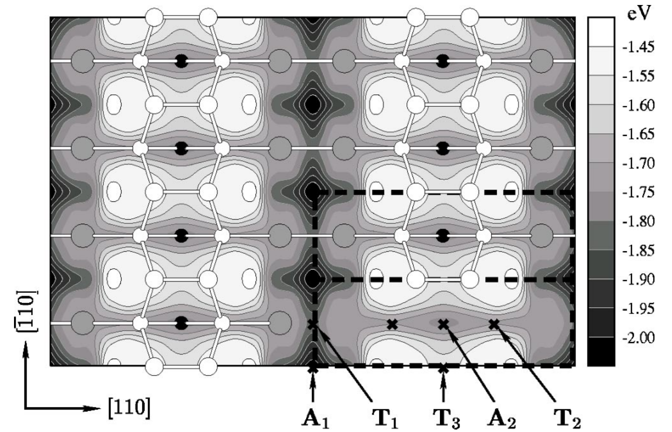

FIG. 6. PES for an In adatom on the $In_{2/3}Ga_{1/3}As(001)$-(1×3) surface, see also Table III. Two unit cells are indicated by dashed rectangles. Overlaid on the PES plot are the topmost three atomic layers (cf. Fig. 1).

$\propto\sqrt{T}$. Here, we are only interested in a qualitative estimate of the importance of double jumps. For this purpose, we do not discuss the temperature dependence of the prefactor, but simply introduce a phenomenological (unknown) equilibration probability $\alpha(T)$ in site $\mathbf{A}_2$ that allows for a rough estimate. The rates of single and double jumps starting from $\mathbf{A}_1$ are assumed to be $\alpha(T)\Gamma_{21}$ and $\tilde{\Gamma}_{11}=[1-\alpha(T)]\Gamma_{21}$, respectively. While $\alpha=1$ corresponds to the case of single jumps only, an upper limit for the effect of double jumps can be obtained by setting $\alpha=0$. More details are given in Appendix A.

Figure 5 shows the temperature dependence of the tracer

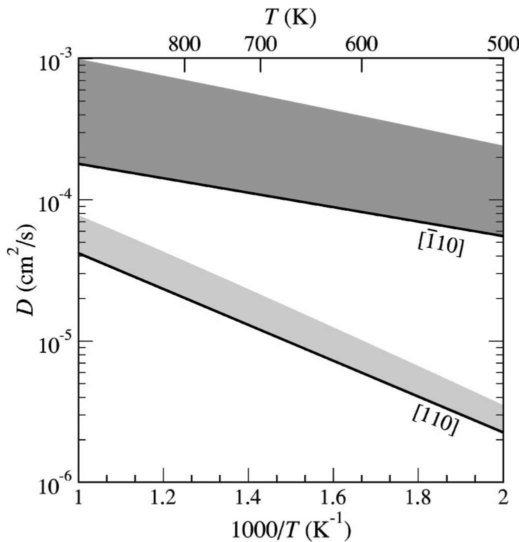

FIG. 5. Tracer diffusion coefficients of an indium adatom on the $In_{2/3}Ga_{1/3}As(001)$-(2×3) surface calculated within the random-walk formalism (Appendix A). The lines refer to the assumption that only single jumps occur, and the shaded regions indicate the maximum enhancement of the diffusivity due to double jumps (see text for more details).

diffusion coefficients. The shaded areas in the plot represent the uncertainty due to the possibility of double jumps, estimated by varying $\alpha(T)$ between zero and unity. The lower boundary of the shaded areas corresponds to the single-jump expressions (A9), and applies in the low-temperature (or high friction and $\epsilon\sim1$) regime. The upper boundaries correspond to the rather extreme, hypothetical case in which *all* jumps along the trench in $[\bar{1}10]$ direction proceed as double jumps. For a realistic estimate knowledge of the friction coefficient is required. We note, however that, unless for very low friction, the barrier $\Delta E_{12}=0.08$ eV is sufficiently high to ensure equilibration of diffusing particles in $\mathbf{A}_2$ for temperatures below $T\simeq600$ K. Only at higher temperatures, contributions from double jumps may become noticeable. The actual behavior of the diffusion coefficients is thus expected to closely follow the line in Fig. 5 representing single jumps at low temperatures, and only at higher temperatures D may start entering the shaded region. As also expected, the wider shaded area in Fig. 5 demonstrates the more pronounced effect of eventual double jumps on $D_{[\bar{1}10]}$ as compared to diffusion along the orthogonal surface direction. It is also noteworthy that $[\bar{1}10]$ is always the faster diffusion direction, although the anisotropy ratio varies with temperature.

B. In adatom on $In_{2/3}Ga_{1/3}As(001)$-(1×3)

The calculated PES for In on the (1×3)-reconstructed surface is shown in Fig. 6. As could be expected, the main differences to the PES in Fig. 2 are associated with the region between the continuous As dimer rows. The most stable adsorption site $\mathbf{A}_1$ is now positioned between the In dimers. Another very shallow potential well $\mathbf{A}_2$ appears, similar to Fig. 2, between the As dimers. The energies at significant points of the PES are collected in Table III.

Additionally, we have calculated the energy at the $\mathbf{T}_1$ site, now allowing for a splitting of the In dimer. Since the difference in binding energy was small compared to the case of an intact dimer bond, the splitting does not lead to the ap-

TABLE III. Binding energy E_b (eV) of an In adatom at significant sites on $In_{2/3}Ga_{1/3}As(001)$-(1×3) surface.

	Site				
	A$_1$	**A**$_2$	**T**$_1$	**T**$_2$	**T**$_3$
E_b	−2.04	−1.76	−1.82	−1.70	−1.57

pearance of a new stable adsorption site. Thus, the PES in Fig. 6 gives a valid description of diffusion, and will be used in the further analysis.

Let us analyze now In migration on such a film. For the PES, Fig. 6, application of the RW formalism is simpler than for the case of the (2×3) reconstruction, as can be also seen from the network shown in Fig. 7. Analytical diffusion coefficients are easily accessible, and a detailed consideration is given in Appendix B, Eq. (B2). The prefactors for single jumps and the related energy barriers are collected in Table IV. Under typical growth conditions, however, from Table IV it is clear that jumps "$2\rightarrow1$" do not meet Eq. (2). The In atoms may no longer equilibrate in the shallow minimum $\mathbf{A}_2$ on top of the As dimer rows, but rather move in *one* long jump in [110] direction from one trench to the next. A rigorous treatment of this situation is given in Appendix B. It is worth noting that, on the basis of the above remark, one can simply eliminate $\mathbf{A}_2$ from the network of binding sites. The task thus reduces to a RW on a rectangular lattice defined by the $\mathbf{A}_1$ sites. A very similar case is that of an indium adatom on the GaAs(001)-$c(4\times4)$ surface discussed in Ref. 19. In analogy to the latter, the transition matrix, Eq. (A3), reduces to a single element

$$\Gamma(\mathbf{q})=2\Gamma_{11}(\cos q-1)+2\tilde{\Gamma}_{11}f(\mathbf{q}), \tag{4}$$

where $\tilde{\Gamma}_{11}$ is the rate of double jumps $\mathbf{A}_1\rightarrow\mathbf{A}_2\rightarrow\mathbf{A}_1$, and $f(\mathbf{q})$ is given by Eq. (B4). It is now straightforward to apply the formalism from Appendix A, which gives

$$D_{[110]}\simeq18a^2\tilde{\Gamma}_{11}, \quad D_{[\bar{1}10]}\simeq\tfrac{1}{2}a^2(\Gamma_{11}+2\tilde{\Gamma}_{11}), \tag{5}$$

and the diffusion anisotropy

$$\frac{D_{[110]}}{D_{[\bar{1}10]}}=18(1+\Gamma_{11}/2\tilde{\Gamma}_{11})^{-1}. \tag{6}$$

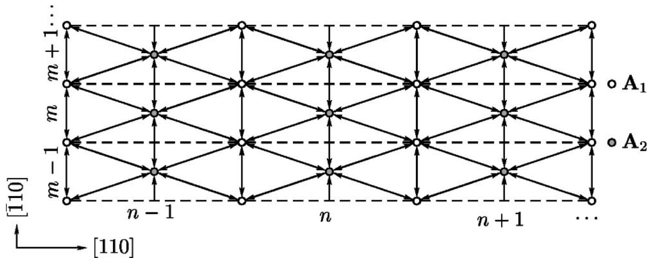

FIG. 7. Network of binding sites ($N_b=2$) for an In adatom on the $In_{2/3}Ga_{1/3}As(001)$-(1×3) surface used in the RW formalism.

TABLE IV. Activation energies ΔE (in eV, according to Table III) and attempt frequencies Γ^0_{fi} (THz) for single jumps on the $In_{2/3}Ga_{1/3}As(001)$-(1×3) surface.

	$fi(\mathbf{A}_i\rightarrow\mathbf{A}_f)$			
	11	12	21	22
ΔE	0.22	0.06	0.34	0.19
Γ^0_{fi}	0.8	0.2	0.6	0.3

Note that $\tilde{\Gamma}_{11}$ appears also in $D_{[\bar{1}10]}$, reflecting the possibility of jump branching: from the $\mathbf{A}_2$ site the In atom can move to either of the two neighboring $\mathbf{A}_1$ sites crossing the same $\mathbf{T}_2$, see Figs. 6 and 7.

The calculated diffusion coefficients are shown in Fig. 8. Again, we use the equilibration probability $\alpha(T)$ to estimate the importance of double jumps. The lower boundary, corresponding to $\alpha=1$, is obtained from Eq. (B2). The upper boundary, $\alpha=0$, results from the inclusion of double jumps according to Eq. (5), where Γ_{21} has been used as an upper limit for $\tilde{\Gamma}_{11}$. We note that the upper boundary of the estimated diffusion coefficient $D_{[110]}$ is a factor 4 higher than the lower boundary, because switching from single to double jumps increases the jump length by a factor of 2, which enters quadratically in the diffusion coefficient. Applying the same arguments as in Sec. III A, we again conclude that the actual diffusion coefficient will closely follow the single-jump limit at low temperatures, while it may somewhat increase above that limit at higher temperatures, but remain within the shaded region in Fig. 8. Thus we establish a qualitatively different behavior of a random walker on the (1×3) surface compared to the (2×3): the faster diffusion direction is found to switch from $[\bar{1}10]$ to [110] upon rais-

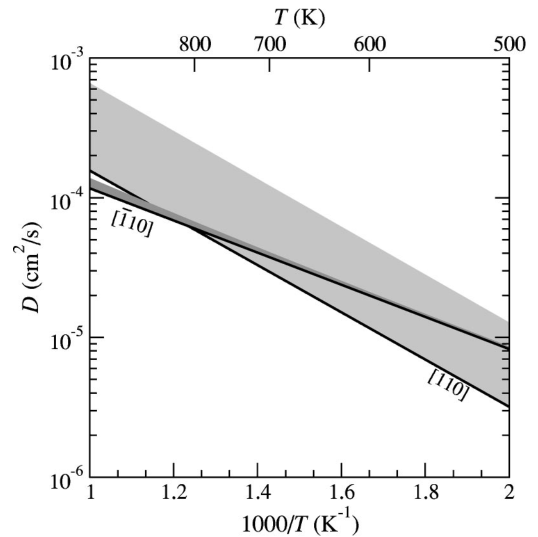

FIG. 8. Tracer diffusion coefficients of an indium adatom on the $In_{2/3}Ga_{1/3}As(001)$-(1×3) surface calculated with the random-walk formalism (Appendix B). The lines refer to the assumption that only single jumps occur, and the shaded regions indicate the maximum enhancement of the diffusivity due to double jumps.

ing the temperature. Double jumps, if possible, contribute almost exclusively to $D_{[110]}$ and affect the actual T of the crossover point. Since the frequency prefactors in Table IV show no clear preference for one diffusion direction, the crossover must be attributed to the larger jump length (three surface lattice constants for double jumps $\mathbf{A}_1 \rightarrow \mathbf{A}_2 \rightarrow \mathbf{A}_1$) in the $[110]$ direction.

IV. DISCUSSION AND CONCLUSIONS

The ultimate implications of the quantitative information obtained from the PES's in Sec. III are best formulated when comparing to the similar analysis of In diffusion on the GaAs(001)-$c(4\times4)$ substrate (three As dimers per unit cell).[19] In Ref. 19 it was found that the diffusion for In on the latter surface is characterized with an energy barrier of 0.65 eV. In contrast, the rate-limiting steps on both the (2×3)- and (1×3)-reconstructed $In_{2/3}Ga_{1/3}As(001)$ film are determined by significantly smaller barriers: on the (2×3)-reconstructed surface, these are 0.13 eV and $\simeq 0.3$ eV in $[\bar{1}10]$ and $[110]$ direction, respectively. On the (1×3) reconstructed surface, diffusion is more isotropic, with energy barriers in the range of 0.2–0.3 eV for both directions. Thus the typical energy scales for the potential-energy surfaces on the bare substrate and the pseudomorphic films turn out clearly different. If we define an onset temperature for diffusion, T^*, by demanding that a single jump should occur at least once per second, i.e.,

$$T^* = \Delta E [k_B \ln(\Gamma^0/\Gamma = 1 \ \mathrm{s}^{-1})]^{-1}, \tag{7}$$

the onset of In diffusion on the $In_{2/3}Ga_{1/3}As(001)$ film in $[110]$ direction occurs at a temperature T^* about 130 K lower than the one on the GaAs(001)-$c(4\times4)$ surface. For diffusion in the $[\bar{1}10]$, the onset temperature on the (2×3)-reconstructed surface is lower by even 190 K, compared to the GaAs(001)-$c(4\times4)$ surface. On the other hand, in all cases attempt frequencies Γ^0 are of the order of terahertz, and their magnitudes are uncorrelated with the barrier heights. Thus we find no evidence for the so-called compensation effect.[51,52] One can therefore predict a considerably higher In mobility on the $In_{2/3}Ga_{1/3}As(001)$ film as compared to the GaAs(001)-$c(4\times4)$ substrate. The cation intermixing in the initial stages of InAs/GaAs(001) heteroepitaxy thus renders the morphology of the growing surface perfectly suited to support substantial mass transport. This finding appears compatible with the experimental reports on In adatom migration in In(Ga)As/GaAs heteroepitaxy. An extremely long In migration length ($\sim 25\ \mu$m) has been derived from measured composition profiles by Arent *et al.*[53] during MBE growth of $In_xGa_{1-x}As$/GaAs with $x = 0.1$–0.22.

One should keep in mind, however, that our theoretical analysis applies to indium diffusion on the ideal infinite surfaces of the respective reconstructions. As established by various experimental techniques, the WL surface is characterized by a substantial structural disorder. In the (2×3) reconstruction the As dimers sitting on the In atoms may largely be missing, which will result locally in the (1×3) reconstruction. The coexistence of $c(4\times4)$ and threefold-reconstructed domains in the very early stages of InAs deposition also should be taken into account. The presence of disorder considerably complicates first-principles calculations of a realistic WL. Yet, its effect can be assessed by kinetic Monte Carlo simulations. This technique has been applied very successfully to the homoepitaxy of metals, and even to the more complicated case of GaAs.[54,27] Our results are thus suitable to serve as an input to such simulations. Future research will therefore be focused on kinetic Monte Carlo simulations of In diffusion on a disordered WL and possible consequences for growth of quantum dots.

ACKNOWLEDGMENTS

This work was supported by the Deutsche Forschungsgemeinschaft within Research Center Sfb 296. S.S. acknowledges support from the Alexander von Humboldt Foundation.

APPENDIX A: DERIVATION OF D FOR INDIUM DIFFUSION ON $In_{2/3}Ga_{1/3}As(001)$-(2×3)

First consider such temperature T that the condition (2) is met for all activation energies in Table II. Hence, one can map the 2D lattice of binding sites determined from Fig. 2 onto the network shown in Fig. 4, representing the uncorrelated adatom jumps to nearest-neighbor sites. Following Refs. 44 and 55, consider a Markovian RW on such an infinite lattice. Then it can be shown that the tracer diffusion tensor D in Cartesian coordinates reads

$$\mathsf{D} = \mathsf{B} \cdot \mathsf{H} \cdot \mathsf{B}^{\mathrm{T}}, \tag{A1}$$

where $\mathsf{B} = (\hat{\mathbf{e}}_m, \hat{\mathbf{e}}_n)$ is the transformation matrix from lattice coordinates to Cartesian coordinates, B^{T}—its transposed, and H the matrix of second derivatives of the longest-living diffusion mode $\gamma(\mathbf{q})$ in the hydrodynamic limit $\mathbf{q} \rightarrow 0$,

$$\mathsf{H}_{\alpha\beta} = -\frac{1}{2} \frac{\partial^2}{\partial q_\alpha \partial q_\beta} \gamma(\mathbf{q}) \bigg|_{\mathbf{q}=0}. \tag{A2}$$

Note that $\gamma(\mathbf{q})$ is the eigenvalue of the Fourier-transformed transition rate matrix that vanishes in the limit[56] $\mathbf{q} \rightarrow 0$

$$\Gamma_{ij}(\mathbf{q}) = \sum_{\mathbf{n}} e^{-i\mathbf{q}\cdot\mathbf{n}} \Gamma_{ij}(\mathbf{n}) - \delta_{ij} \sum_{k=1}^{N_b} \sum_{\mathbf{n}} \Gamma_{ki}(\mathbf{n}), \tag{A3}$$

where $\mathbf{n} = (n,m)$ is the vector index labeling the unit cell, Fig. 4, N_b the number of binding sites per unit cell, and δ_{ij} is the Kronecker delta. In practical applications one does not directly approach the full $N_b \times N_b$ eigenvalue problem for $\Gamma(\mathbf{q})$. Instead, exploiting the smallness of γ in the hydrodynamic limit it is justified to work out the characteristic polynomial of $\Gamma(\mathbf{q})$ up to terms linear in γ,

$$\sum_{n=0}^{N_b} a_n \gamma^n \simeq a_0(\mathbf{q}) + a_1(\mathbf{q}) \gamma(\mathbf{q}) + O(\gamma^2) = 0. \tag{A4}$$

Substituting γ from Eq. (A4) into Eq. (A2), an approximate expression for H follows:

$$\mathsf{H}_{\alpha\beta} \simeq -\frac{1}{2a_1(\mathbf{0})}\frac{\partial^2}{\partial q_\alpha \partial q_\beta} a_0(\mathbf{q})\bigg|_{\mathbf{q}=0}. \tag{A5}$$

For the case of the (2×3) lattice in Fig. 4, $\Gamma(\mathbf{q})$ reads

$$\Gamma(\mathbf{q}) = \begin{pmatrix} -\Sigma_1 & e^{ip}\Gamma_{11} & (1+e^{-iq})\Gamma_{12} & 0 & \Gamma_{13} & \Gamma_{13} \\ e^{-ip}\Gamma_{11} & -\Sigma_1 & 0 & (1+e^{-iq})\Gamma_{12} & \Gamma_{13} & \Gamma_{13} \\ (1+e^{iq})\Gamma_{21} & 0 & -\Sigma_2 & e^{ip}\Gamma_{22} & 0 & 0 \\ 0 & (1+e^{iq})\Gamma_{21} & e^{-ip}\Gamma_{22} & -\Sigma_2 & 0 & 0 \\ \Gamma_{31} & \Gamma_{31} & 0 & 0 & -2\Sigma_3 & (1+e^{iq})\Gamma_{33} \\ \Gamma_{31} & \Gamma_{31} & 0 & 0 & (1+e^{-iq})\Gamma_{33} & -2\Sigma_3 \end{pmatrix}, \tag{A6}$$

where $\mathbf{q}=(p,q)$, and the diagonal terms are given by

$$\Sigma_1 = \Gamma_{11} + 2\Gamma_{21} + 2\Gamma_{31}, \quad \Sigma_2 = 2\Gamma_{12} + \Gamma_{22} + 2\Gamma_{32}, \quad \Sigma_3 = \Gamma_{13} + \Gamma_{23} + \Gamma_{33}. \tag{A7}$$

Now taking into account that $\mathsf{B}=(a/\sqrt{2})\begin{pmatrix}3 & 0\\ 0 & 2\end{pmatrix}$, where a is the bulk lattice constant of GaAs, the tracer diffusion tensor

$$\mathsf{D} = \begin{pmatrix} D_{[110]} & 0 \\ 0 & D_{[\bar{1}10]} \end{pmatrix} \tag{A8}$$

can be obtained from Eqs. (A6), (A4), (A5), and (A1):

$$D_{[110]} \simeq \frac{9\Gamma_{12}\Gamma_{13}\Gamma_{31}[\Gamma_{21}\Gamma_{22} + \Gamma_{11}(\Gamma_{12}+\Gamma_{22})]}{4[\Gamma_{21}\Gamma_{22} + \Gamma_{11}(\Gamma_{12}+\Gamma_{22}) + \Gamma_{31}(\Gamma_{12}+\Gamma_{22})][\Gamma_{13}\Gamma_{21} + \Gamma_{12}(\Gamma_{13}+\Gamma_{31})]} a^2,$$

$$D_{[\bar{1}10]} \simeq \frac{\Gamma_{12}[\Gamma_{21}\Gamma_{13}^2 + (2\Gamma_{21}+\Gamma_{31})\Gamma_{33}\Gamma_{13} + 3\Gamma_{31}\Gamma_{33}^2]}{[\Gamma_{13}\Gamma_{21} + \Gamma_{12}(\Gamma_{13}+\Gamma_{31})][\Gamma_{13}+2\Gamma_{33}]} a^2. \tag{A9}$$

Now let us consider the case where not all activation energies obey Eq. (2). As seen from Table II for the (2×3) reconstruction this can readily occur for hops from $\mathbf{A}_2$ to $\mathbf{A}_1$ for which the activation energy is only 80 meV. Hence, in the simplest case, the energy dissipated by the adatom along the path section $\mathbf{T}_1 \to \mathbf{A}_2 \to \mathbf{T}_1$, may be low enough as to allow for double jumps $\mathbf{A}_1 \to \mathbf{A}_2 \to \mathbf{A}_1$ say at rate $\tilde{\Gamma}_{11}$. Note that the latter quantity is not directly accessible within transition state theory; a practical procedure has been developed, e.g., in Refs. 38–40.

Following the same steps when deriving Eq. (A6) it is easy to show that inclusion of terms $\propto \tilde{\Gamma}_{11}$ "renormalizes" only Σ_1 in Eq. (A6), $\Sigma_1 \to \Sigma_1 - 2\tilde{\Gamma}_{11}(\cos q - 1)$. Then the same previous expressions can be used to obtain the correction to the diffusion coefficients.

APPENDIX B: DERIVATION OF D FOR INDIUM DIFFUSION ON $In_{2/3}Ga_{1/3}As(001)$-(1×3)

In analogy to the case in Appendix A, consider first a temperature range where the fully connected network shown in Fig. 7 is applicable to In surface migration on the (1×3) PES, Fig. 6. The analytical procedure is now much simpler, as $N_b=2$ and the corresponding Fourier-transformed transition rate matrix takes the simple form

$$\Gamma(\mathbf{q}) = \begin{pmatrix} 2[\Gamma_{11}(\cos q - 1) - 2\Gamma_{21}] & (1+e^{ip}+e^{iq}+e^{i(p+q)})\Gamma_{12} \\ (1+e^{-ip}+e^{-iq}+e^{-i(p+q)})\Gamma_{21} & 2[\Gamma_{22}(\cos q - 1) - 2\Gamma_{12}] \end{pmatrix}. \tag{B1}$$

Using the coordinate transformation matrix $\mathsf{B}=(a/\sqrt{2})\begin{pmatrix}3 & 0\\ 0 & 1\end{pmatrix}$, it is possible to obtain explicit expressions for the indium tracer diffusion coefficients, Eq. (A8), on the $In_{2/3}Ga_{1/3}As(001)$-(1×3) surface,

$$D_{[110]} \simeq 9a^2 \frac{\Gamma_{12}\Gamma_{21}}{2(\Gamma_{12}+\Gamma_{21})}, \qquad D_{[\bar{1}10]} \simeq a^2 \frac{\Gamma_{11}\Gamma_{12} + \Gamma_{21}(\Gamma_{12}+\Gamma_{22})}{2(\Gamma_{12}+\Gamma_{21})}. \tag{B2}$$

The quotient of these expressions gives the diffusion anisotropy

$$\frac{D_{[110]}}{D_{[\bar{1}10]}}=9\left(1+\frac{\Gamma_{11}}{\Gamma_{21}}+\frac{\Gamma_{22}}{\Gamma_{12}}\right)^{-1}. \tag{B3}$$

Consider now a modified jump motion including double jumps $\mathbf{A}_1\rightarrow\mathbf{A}_2\rightarrow\mathbf{A}_1$ which may easily occur because of the very low activation energy (60 meV, see Table IV) required for the transition from $\mathbf{A}_2$ to a neighboring $\mathbf{A}_1$ site. The corresponding $\Gamma(\mathbf{q})$ matrix is similar to Eq. (B1) where only the $\Gamma_{11}(\mathbf{q})$ element is modified, $\Gamma_{11}(\mathbf{q})\rightarrow\Gamma_{11}(\mathbf{q})+f(\mathbf{q})\tilde{\Gamma}_{11}$,

$$f(\mathbf{q})=2\cos p+\cos(p+q)+\cos(p-q)-4, \tag{B4}$$

and $\tilde{\Gamma}_{11}$ is the rate of the double-jump process. Corrections to the diffusion coefficients (B2) can be easily worked out noting that $f(0)=0$, $\nabla_{\mathbf{q}}f(\mathbf{q})|_0=0$, and that mixed second derivatives of f also vanish in the limit $\mathbf{q}\rightarrow 0$. Hence, denoting these corrections $D^{(2)}$, Eq. (B2) is modified by adding, respectively, the terms

$$D^{(2)}_{[110]}\simeq 9a^2\frac{2\Gamma_{12}\tilde{\Gamma}_{11}}{\Gamma_{12}+\Gamma_{21}},$$

$$D^{(2)}_{[\bar{1}10]}\simeq a^2\frac{\Gamma_{12}\tilde{\Gamma}_{11}}{\Gamma_{12}+\Gamma_{21}}. \tag{B5}$$

*Present address: CEMES/CNRS, 29, rue Jeanne Marvig, B.P. 4347, 31055 Toulouse Cedex, France.

[1] Y.-W. Mo, J. Kleiner, M.B. Webb, and M.G. Lagally, Phys. Rev. Lett. **66**, 1998 (1991).
[2] Y.-W. Mo, J. Kleiner, M.B. Webb, and M.G. Lagally, Surf. Sci. **268**, 275 (1992).
[3] B. Voigtlander and T. Weber, Phys. Rev. Lett. **77**, 3861 (1996).
[4] B. Voigtlander and M. Kastner, Surf. Sci. **464**, 131 (2000); Appl. Phys. A: Mater. Sci. Process. **63**, 577 (1997).
[5] R. Gomer, Rep. Prog. Phys. **53**, 917 (1990), and references therein.
[6] T. Ala-Nissila, R. Ferrando, and S.C. Ying, Adv. Phys. **51**, 949 (2002), and references therein.
[7] S. Guha, A. Madhukar, and K.C. Rajkumar, Appl. Phys. Lett. **57**, 2110 (1990).
[8] J.M. Moison, F. Houzay, F. Barthe, L. Leprince, E. André, and O. Vatel, Appl. Phys. Lett. **64**, 196 (1994).
[9] D. Leonard, K. Pond, and P.M. Petroff, Phys. Rev. B **50**, 11687 (1994).
[10] P. Kratzer, C. Morgan, and M. Scheffler, Prog. Surf. Sci. **59**, 135 (1998).
[11] L.G. Wang, P. Kratzer, N. Moll, and M. Scheffler, Phys. Rev. B **62**, 1897 (2000).
[12] T.R. Ramachandran, R. Heitz, P. Chen, and A. Madhukar, Appl. Phys. Lett. **70**, 640 (1997).
[13] T.R. Ramachandran, A. Madhukar, I. Mukhametzhanov, R. Heitz, A. Kalburge, Q. Xie, and P. Chen, J. Vac. Sci. Technol. B **16**, 1330 (1998).
[14] B.A. Joyce, D.D. Vvedensky, A.R. Avery, J.G. Belk, H.T. Dobbs, and T. Jones, Appl. Surf. Sci. **130-132**, 357 (1998).
[15] P.B. Joyce, T.J. Krzyzewski, G.R. Bell, B.A. Joyce, and T.S. Jones, Phys. Rev. B **58**, R15 981 (1998).
[16] B.A. Joyce, D.D. Vvedensky, T.S. Jones, M. Itoh, G.R. Bell, and J. Belk, J. Cryst. Growth **201/202**, 106 (1999).
[17] F. Patella, M. Fantofi, F. Arciprete, S. Nufris, E. Placidi, and A. Balzarotti, Appl. Phys. Lett. **78**, 320 (2001).
[18] A. Rosenauer, D. Gerthsen, D. VanDyck, M. Arzberger, G. Böhm, and G. Abstreiter, Phys. Rev. B **64**, 245334 (2001).
[19] E. Penev, P. Kratzer, and M. Scheffler, Phys. Rev. B **64**, 085401 (2001).
[20] P. Kratzer, E. Penev, and M. Scheffler, Appl. Phys. A: Mater. Sci. Process. **75**, 79 (2002).
[21] D.K. Biegelsen, R.D. Bringans, J.E. Northrup, and L.-E. Swartz, Phys. Rev. B **41**, 5701 (1990).
[22] M. Sauvage-Simkin, R. Pinchaux, J. Massies, P. Claverie, N. Jedrecy, J. Bonnet, and I.K. Robinson, Phys. Rev. Lett. **62**, 563 (1989).
[23] M. Sauvage-Simkin, Y. Garreau, R. Pinchaux, M.B. Véron, J.P. Landesman, and J. Nagle, Phys. Rev. Lett. **75**, 3485 (1995).
[24] M. Sauvage-Simkin, Y. Garreau, R. Pinchaux, A. Cavanna, M.B. Véron, N. Jedrecy, J.P. Landesman, and J. Nagle, Appl. Surf. Sci. **104/105**, 646 (1996).
[25] J.G. Belk, C.F. McConville, J.L. Sudijono, T.S. Jones, and B.A. Joyce, Surf. Sci. **387**, 213 (1997).
[26] E. Penev, P. Kratzer, and M. Scheffler (unpublished).
[27] P. Kratzer, E. Penev, and M. Scheffler, Appl. Surf. Sci. **216**, 436 (2003).
[28] Y. Garreau, K. Aïd, M. Sauvage-Simkin, R. Pinchaux, C.F. McConville, T.S. Jones, J.L. Sudijono, and E.S. Tok, Phys. Rev. B **58**, 16177 (1998).
[29] P. Kratzer and M. Scheffler, Comput. Sci. Eng. **3**, 16 (2001).
[30] M. Scheffler and P. Kratzer, in *Atomistic Aspects of Epitaxial Growth*, Vol. 65 of *NATO Science, Series II: Mathematics, Physics, and Chemistry*, edited by M. Kotrla, N. I. Papanicolaou, D. D. Vvedensky, and L. T. Wille (Kluwer Academic, Dordrecht, 2002), pp. 355–369.
[31] E. S. Penev, Ph.D. thesis, Technische Universität Berlin, Berlin, 2002, http://www.fhi-berlin.mpg.de/th/publications/PhD-penev-2002.pdf
[32] M. Bockstedte, A. Kley, J. Neugebauer, and M. Scheffler, Comput. Phys. Commun. **107**, 187 (1997), http://www.fhi-berlin.mpg.de/th/fhimd
[33] J.P. Perdew, K. Burke, and M. Ernzerhof, Phys. Rev. Lett. **77**, 3865 (1996).
[34] M. Fuchs and M. Scheffler, Comput. Phys. Commun. **119**, 67 (1999), http://www.fhi-berlin.mpg.de/th/fhi98md/fhi98PP/
[35] A. Preusser, ACM Trans. Math. Softw. **15**, 79 (1989), http://www.fhi-berlin.mpg.de/grz/pub/xfarbe/
[36] P. Hänggi, P. Talkner, and M. Borkovec, Rev. Mod. Phys. **62**, 251 (1990), and references therein.
[37] C. Ratsch and M. Scheffler, Phys. Rev. B **58**, 13163 (1998).
[38] R. Ferrando, R. Spadacini, and G.E. Tommei, Phys. Rev. E **48**, 2437 (1993); R. Ferrando, R. Spadacini, G.E. Tommei, and G. Caratti, Surf. Sci. **311**, 411 (1994); F. Montalenti and R. Ferrando, Phys. Rev. B **59**, 5881 (1999); O.M. Braun and

R. Ferrando, Phys. Rev. E **65**, 061107 (2002).

[39] E. Hershkovitz, P. Talkner, E. Pollak, and Y. Georgievskii, Surf. Sci. **421**, 73 (1999); Y. Georgievskii and E. Pollak, *ibid.* **355**, L366 (1996); Y. Georgievskii, M.A. Kozhushner, and E. Pollak, J. Chem. Phys. **102**, 6908 (1995); Y. Georgievskii and E. Pollak, Phys. Rev. E **49**, 5098 (1994).

[40] J. Jacobsen, K.W. Jacobsen, and J.P. Sethna, Phys. Rev. Lett. **79**, 2843 (1997).

[41] A theoretical scheme to obtain a rough estimate for the friction coefficient in the phononic dissipation channel is given, e.g., by B.N.J. Persson and R. Ryberg, Phys. Rev. B **32**, 3586 (1985).

[42] J.D. Wrigley, M.E. Twigg, and G. Ehrlich, J. Chem. Phys. **93**, 2885 (1990).

[43] R. Festa and E. Galleani d'Agliano, Physica A **90**, 229 (1978).

[44] A. Natori and R.W. Godby, Phys. Rev. B **47**, 15816 (1993).

[45] A. Kley, P. Ruggerone, and M. Scheffler, Phys. Rev. Lett. **79**, 5278 (1997).

[46] L. Bellaiche, K. Kunc, M. Sauvage-Simkin, Y. Garreau, and R. Pinchaux, Phys. Rev. B **53**, 7417 (1996).

[47] T. Kita, O. Wada, T. Nakayama, and M. Murayama, Phys. Rev. B **66**, 195312 (2002).

[48] I. Kamiya, D.E. Aspnes, L.T. Florez, and J.P. Harbison, Phys. Rev. B **46**, 15894 (1992).

[49] P. Kratzer, C.G. Morgan, and M. Scheffler, Phys. Rev. B **59**, 15 246 (1999).

[50] I.V. Ionova and E.A. Carter, J. Chem. Phys. **98**, 6377 (1993); see also E. Penev, P. Kratzer, and M. Scheffler, *ibid.* **110**, 3986 (1999); all spatial degrees of freedom of the atoms in the topmost five layers have been included in the transition-state search. An alternative but computationally more demanding way is to map the PES for an In adatom interacting with the As dimer in the configurational space spanning the As-As distance d and the adatom height Z_{In} above the dimer midpoint (Ref. 19). Here we have performed tests only along the contour line $Z_{\mathrm{In}}^2 + d^2/4 = \mathrm{const}$ [with the constant corresponding to the squared adatom-As bond length in the configuration of Fig. 3(c)], using the constrained relaxation scheme of Ref. 19, and found a very similar energy barrier.

[51] G. Boisvert, L.J. Lewis, and A. Yelon, Phys. Rev. Lett. **75**, 469 (1995).

[52] D. J. Fisher, *The Meyer-Neldel Rule*, Defect and Diffusion Forum Vols. 192 and 193 (Trans Tech, Uetikon-Zürich, 2001).

[53] D. Arent, S. Nilsson, Y. Galeuchet, H. Meier, and W. Walter, Appl. Phys. Lett. **55**, 2611 (1989); see also K.R. Evans, C.E. Stutz, D.K. Lorance, and R.L. Jones, J. Vac. Sci. Technol. B **7**, 259 (1989).

[54] P. Kratzer and M. Scheffler, Phys. Rev. Lett. **88**, 036102 (2002).

[55] A. Kley, *Theoretische Untersuchungen zur Adatomdiffusion auf Niederindizierten Oberflächen von GaAs* (Wissenschaft & Technik Verlag, Berlin, 1997).

[56] J.W. Haus and K.W. Kehr, Phys. Rep. **150**, 263 (1987).